Geologic Hazards Science Center
U.S. Geological Survey
Golden, Colorado
http://landslides.usgs.gov/

USGS science for a changing world

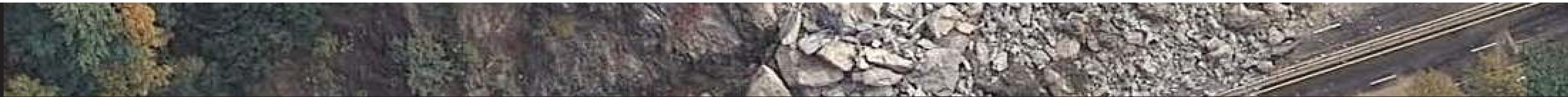

Assessment of potential hurricane-induced shallow landslide sources for Naranjito Municipality, Puerto Rico

CONNECTS 2021 10–13 October Portland, Oregon, USA

Session T-42, Booth 20

Rex L. Baum[1], Dianne L. Brien[2],
Adrian C. Lewis[1], Emily C. Bedinger[1],
William H. Schulz[1], Mark E. Reid[2]
[1]U.S. Geological Survey, Box 25046, Federal Center, Denver, CO 80225
[2]U.S. Geological Survey, P.O. Box 158, Moffat Field, CA 94035

Abstract

Here we describe the landslide initiation (source area) part of a landslide susceptibility assessment of Naranjito Municipality, Puerto Rico. Determining landslide initiation potential is part of an effort to determine debris-flow runout hazard for areas of Puerto Rico affected by Hurricane Maria. A nonlinear area and slope dependent (NASD) soil depth model and the Transient Rainfall Infiltration and Grid-Based Regional Slope-Stability Analysis (TRIGRS) applied across a high-resolution digital landscape show where shallow landslides are likely to initiate during future hurricanes. Soil texture and strength data aided model calibration against detailed event mapping. Slope-stability analysis varying cohesion and friction defined valid ranges of these soil strength parameters for landslide source slope and depth distributions derived from mapping and field studies. Subdividing the map area into geologically based parameter zones distinguished areas where average soil depth or strength differed from other map units (granitic bedrock or karstic limestone, respectively). Statistical comparison of results from 9 different soil models coded in the REGOLITH soil-depth software, each sampled over its respective parameter space, yielded a best fit to field-measured soil depth in landslide scars. Full saturation with the water table at the ground surface and (topographic) slope-parallel flow embodied the most likely hydrologic conditions for landslide initiation. We refined the extent of potential shallow landslide source areas from TRIGRS using a simplified 3-D slope stability analysis, which eliminated many false positives and narrowed the factor of safety, FS, ranges containing 75% and 90% of scarp points. Receiver Operator Characteristics (ROC) analysis of computed FS ranked the predictive success in identifying head-scarp points. The True Positive Rate for FS=1 was reasonable using the chosen soil strength parameters. Susceptibility categories capture 75% (FS=1.12) and 90% (FS=1.22) of the points, with FS ≤ 1.12, high; 1.12 < FS ≤ 1.22, medium, and 1.22 < FS, low susceptibility. The high susceptibility category, with > 48 scarp points/km^2, covers ~30% of the area. The source area susceptibility results provide the input for assessment of runout zones for highly mobile Hurricane Maria landslides.

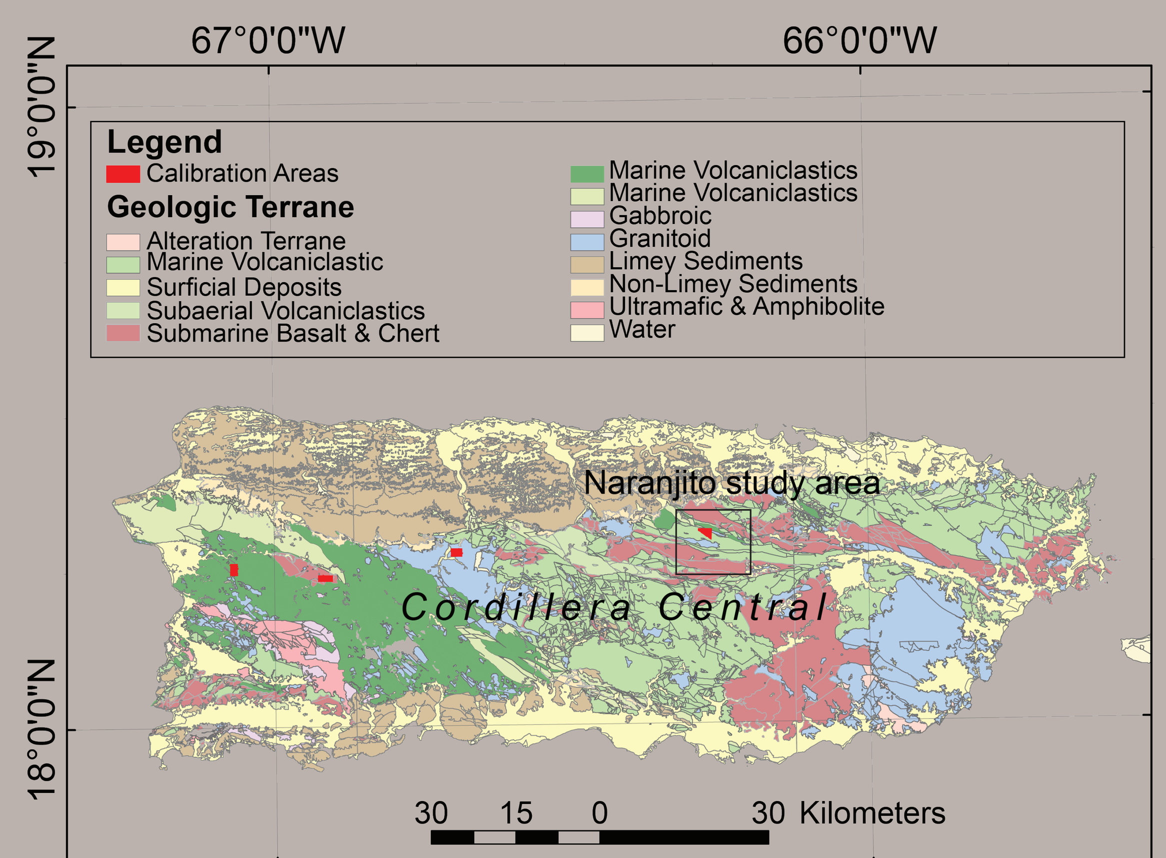

Figure 1. Location of study area overlain on geologic terrane map (Bawiec, 1998).

1. Study Area

Puerto Rico lies at the east end of the Greater Antilles and is characterized by rugged topography. The study area and calibration areas lie in the east–west-trending Cordillera Central range (Fig. 1). Heavily faulted basement rocks, consisting mainly of oceanic crust, and volcaniclastic and intrusive rocks, underlie the range (Jolly et al. 1998).

Bawiec (1998) generalized the geology of Puerto Rico into 12 geologic terranes having related rock types (Fig. 1). Bessette-Kirton et al. (2019a) identified calibration areas in three geologic terranes (igneous intrusive, volcaniclastic, and submarine basalt and chert) where high densities of debris flows occurred. High densities of Hurricane María-induced landslides also were correlated to high antecedent soil moisture (Bessette-Kirton, et al. 2019b).

2. Field study

Observations and measurements of the size, shape, geologic materials, topographic setting, and other characteristics of landslide and debris-flow sources were collected in field studies (Baum et al. 2018, Bessette-Kirton et al. 2019b) (Fig. 2).

Figure 2. Source areas of shallow landslides in volcaniclastic terrane (left) and igneous intrusive terrane (rigt) (C. Cerovski-Darriau, USGS).

3. Parameter testing

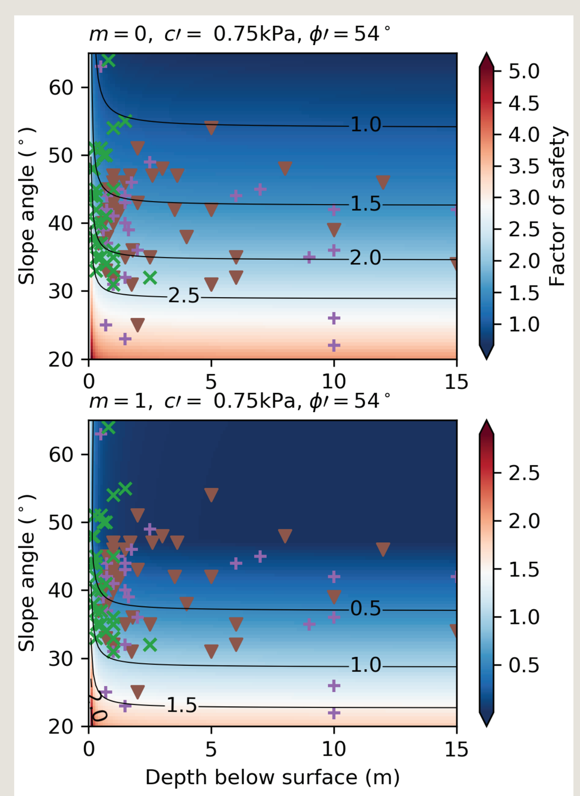

Figure 3. Factor of safety results for combination of cohesion, c′, angle of internal friction, ϕ′, and pore-pressure head, where *m* is the ratio of pore-pressure head to soil depth. Observed slope angle and depth at mapped landslide sources in various geologic terranes, green "x" granitoid intrusive; violet "+" submarine basalt; brown triangle, volcaniclastic. Factor of safety, FS, at slope and depth combinations observed at landslide sources indicates model success (FS<1 if *m*=1) or failure (FS>1 if *m*=1). For the pair of c′ and ϕ′ values shown, FS>1 for dry conditions (*m*=0) at about 97% of sources and FS>1 at 4% of sources for water table at the ground surface with flow parallel to the slope (*m*=1). These parameters, c′ = 0.75 kPa and ϕ′ = 54°, had an overall success rate of about 93% for all three terranes (after Baum 2021).

4. Calibration

We analyzed many possible combinations of cohesion, *c*′, and friction angle, ϕ′, over the observed range of slope and depth of landslide sources (Fig. 3). Compiling the performance of every c′-ϕ′ pair like that in Fig. 3 led to Fig. 4, which showed the better-performing ranges of c′ and ϕ′ overall and for specific geologic terranes. These ranges were used in computing the factor of safety with trial soil-depth maps (Fig. 5) to find the best soil-depth map and c′-ϕ′ combination for each terrane.

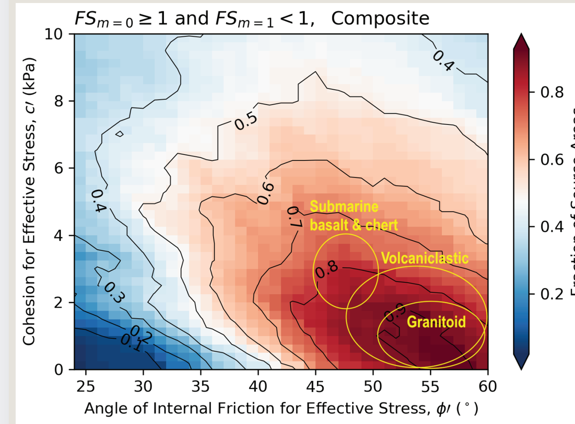

Figure 4. Composite fraction of landslide sources predicted correctly as a function of cohesion, *c*′, and angle of internal friction, ϕ′, for three major bedrock types in Puerto Rico. Each pixel summarizes the net result of a pair of analyses like that in Fig. 3. Yellow ovals show approximate ranges of most successful predictions for each terrane. Factor of safety (FS) for dry conditions is $FS_{m=0}$; factor of safety for water table at ground surface with slope-parallel flow is $FS_{m=1}$. Each grid cell represents the fraction $(NFS_{m=0} – NFS_{m=1})/Nt$, where $NFS_{m=0}$ is the number of source areas for $FS_{m=0}$>=1, $NFS_{m=1}$ is the number of source areas for which $FS_{m=1}$ >=1, and Nt is the number of source areas in the bedrock type (after Baum 2021).

We generated trial soil maps (Fig. 5) for simple empirical and process-based soil-depth models. The trial maps were compared against observed landslide depths to obtain the best fit for each model type (Tello 2020). Then computing factor of safety, FS-1D, for each best-fit soil map and better-performing range of *c*′ and ϕ′ (Fig. 4) and comparing FS-1D with the locations of landslides using Receiver Operator Characteristics (ROC) analysis (Beguria, 2006), showed which of all the best-fit soil models and which c′-ϕ′ combination were the most accurate predictor of landslides for each terrane.

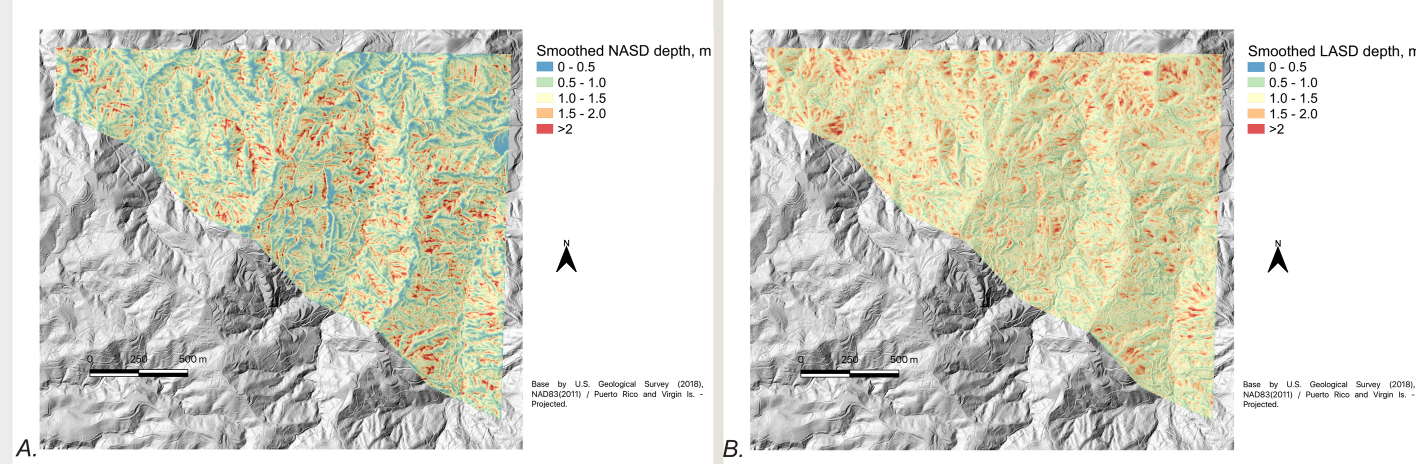

Figure 5. Trial soil maps for two of nine soil-depth models tested for the (triangluar red) calibration area (Fig. 1). (*A*) Best-fit version of the Modified Nonlinear Area and Slope-dependent (NASD) model (Pelletier & Rasmussen, 2009), (*B*) Linear area and slope dependent model based on wetness index (Ho et al. 2012). The NASD model (A) was ultimately chosen as the overall best-fitting soil-depth model for this terrane (volcaniclastic).

5. Modeling

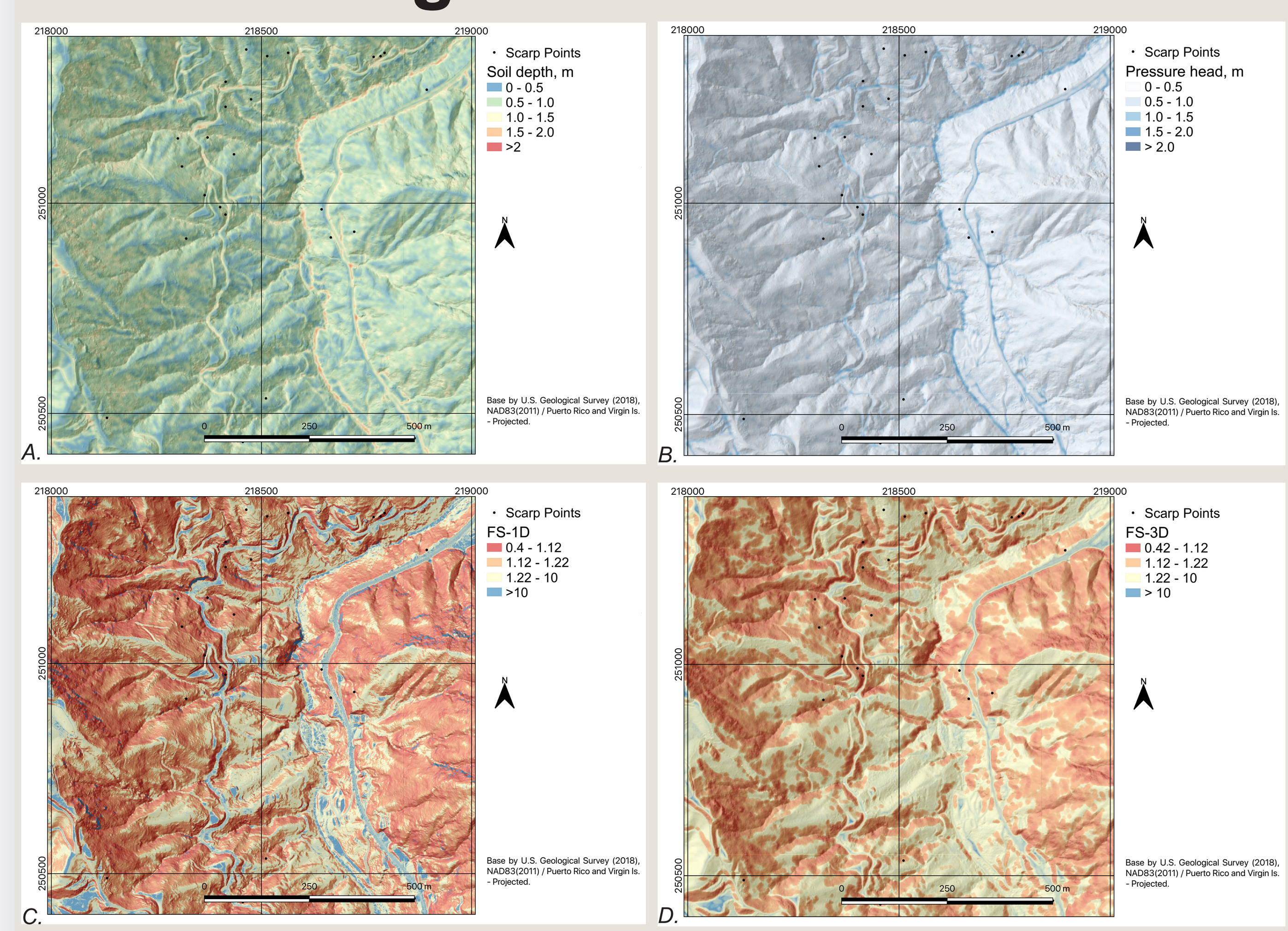

Figure 6. Modeling steps depicted through close-up view of maps of (*A*) soil-depth based on modified non-linear area and slope dependent model (NASD), (*B*) pore-pressure head assuming slope-parallel flow with water table at the ground surface, (*C*) 1-D factor of safety from TRIGRS 2.1 (Alvioli & Baum 2016), (*D*) simplified 3-D factor of safety (Baum et al. 2012).

6. Results

After calibrating the soil-depth models and strength parameters to find the best fit, we computed soil depth, pore-pressure head and 1D factor of safety (FS-1D) for the entire study area. We also used pore-pressure head as input to compute simplified 3D factor of safety (FS-3D). Fig. 6 depicts close-up views of these four outputs and Fig. 7 depicts FS-3D for the entire study area, with a aquaredepicting the area of the close-up (Fig. 6). Fig. 8 depicts FS-3D with an overlay of scarp points (Hughes et al. 2019)

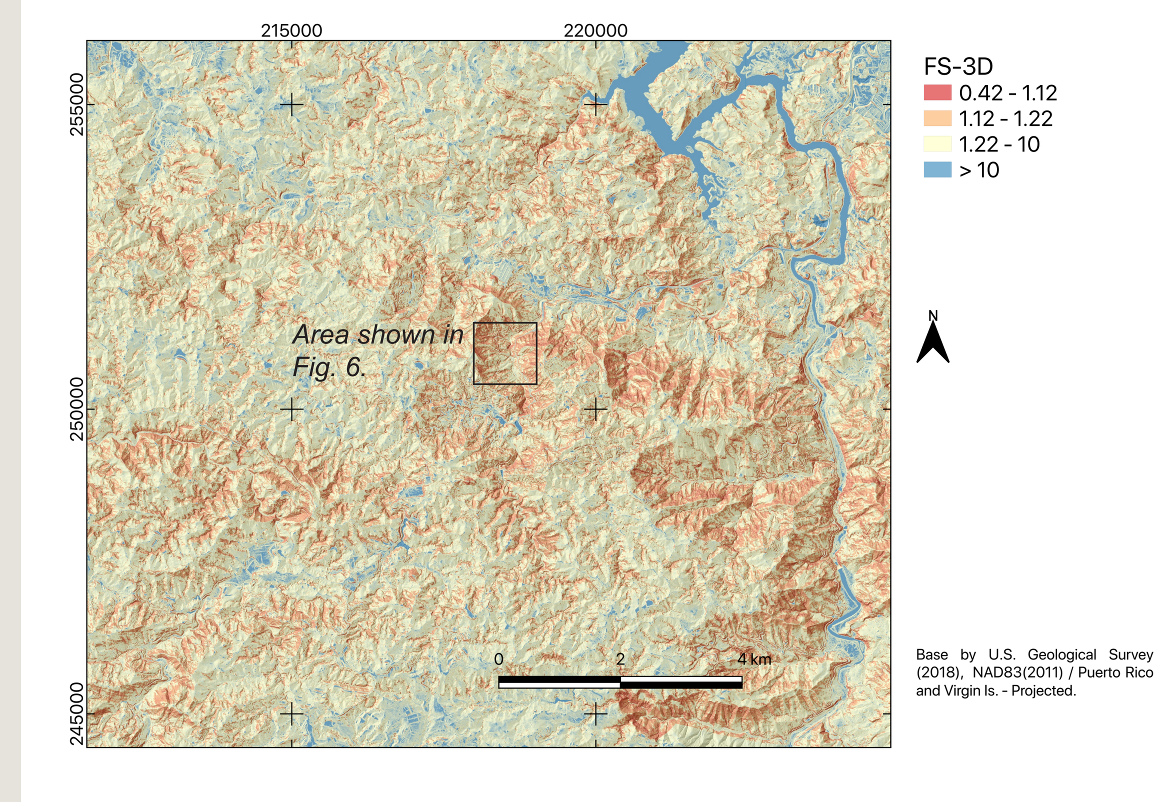

Figure 7. Final map of factor of safety for simplified 3-D slope stability analysis. FS-3D < 1.12 encloses 75% of Hughes et al. (2019) scarp points, FS-3D < 1.22 encloses 90% and FS-3D < 1.30 encloses 95%. The map extends well beyond the limits of Naranjito Municipality so that all drainage basins crossing the Municipality boundaries are complete. This is to ensure that all potential source areas are accounted for in modeling debris-flow transport (Brien et al. 2021).

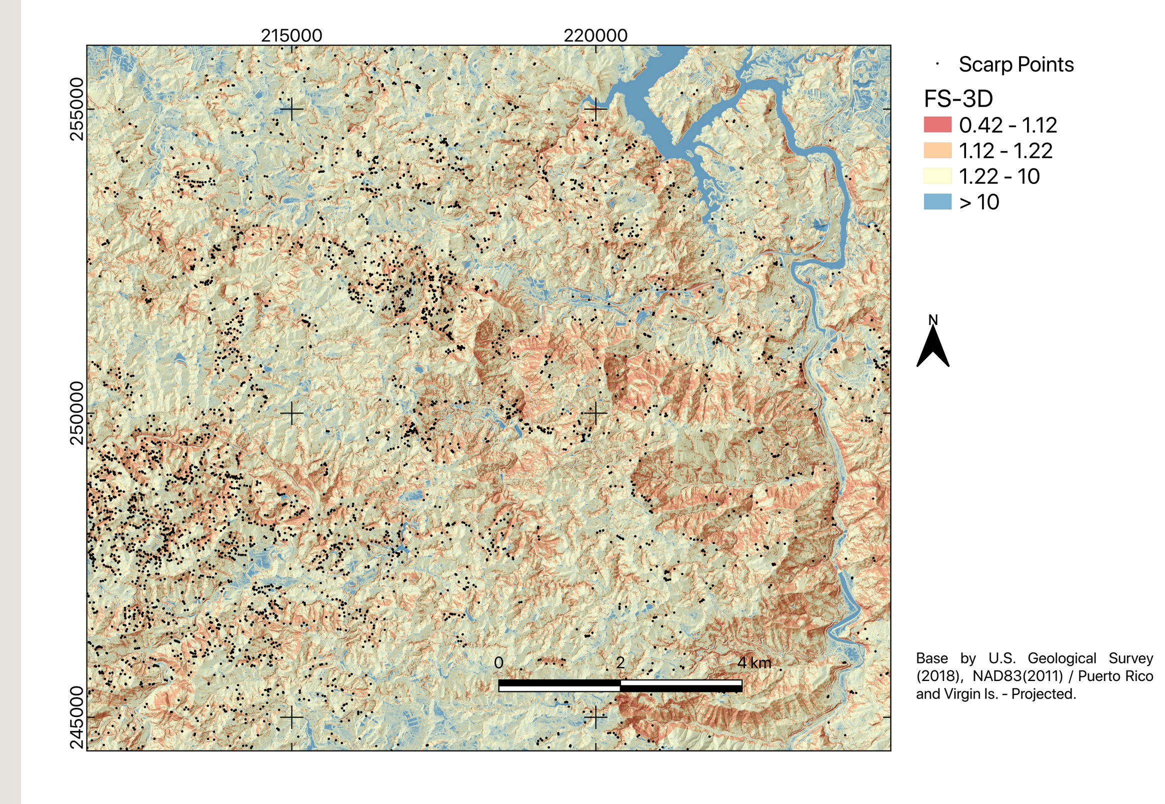

Figure 8. Final map of factor of safety for simplified 3-D slope stability analysis, FS-3D, with overlay of Hughes et al. (2019) scarp points. Although areas of high landslide density occur in areas of low FS-3D, not all susceptible areas were equally affected. Factors such as antecedent soil wetness are known to have affected the density of landslides induced by Hurricane Maria (Bessette-Kirton et al. 2019b).

7. References cited

Alvioli, M., Baum, R.L., 2016, Parallelization of the TRIGRS model for rainfall-induced landslides using the message passing interface. Environmental Modelling & Software 81:122–135. https://doi.org/10.1016/j. envsoft.2016.04.002

Baum, R.L. Godt, J.W. Coe, J.A. and Reid, M.E., 2012, Assessment of shallow landslide potential using 1-D and 3-D slope stability analysis, in Eberhardt, E. Froese, C., Turner, A.K., and Leroueil, S. (eds), Landslides and Engineered Slopes: Protecting Society through Improved Understanding: London, Taylor & Francis Group, p. 1667 - 1672.

Baum R.L., Cerovski-Darriau C., Schulz W.H., Bessette-Kirton E., Coe J.A., Smith J.B., Smoczyk G.M. 2018, Variability of hurricane María debris-flow source areas in Puerto Rico—implications for hazard assessment, abstract NH14A-02 presented at 2018 fall meeting, AGU, Washington, DC, 10–14 Dec., https://abstractsearch.agu.org/ meetings/2018/FM/NH14A-02.html

Baum, R.L. 2021, Rapid Sensitivity Analysis for Reducing Uncertainty in Landslide Hazard Assessments. In: Guzzetti F., Mihalić Arbanas S., Reichenbach P., Sassa K., Bobrowsky P.T., Takara K. (eds) Understanding and Reducing Landslide Disaster Risk. WLF 2020. ICL Contribution to Landslide Disaster Risk Reduction. Springer, Cham. https://doi.org/10.1007/978-3-030-60227-7_37

Bawiec, W.J., 1998, Geologic terranes of Puerto Rico, In: Bawiec, W.J. (ed) Geology, geochemistry, geophysics, mineral occurrences and mineral resource assessment for the commonwealth of Puerto Rico: U.S. Geological Survey Open-File Report 98–38. https://doi.org/10. 3133/ofr9838

Begueria, S., 2006, Validation and evaluation of predictive models in hazard assessment and risk management: Natural Hazards, v. 37, p. 315–329, accessed June 21, 2016, at https://doi.org/10.1007/s11069-005-5182-6.

Bessette-Kirton E.K., Coe J.A., Kelly M.A., Cerovski-Darriau C., Schulz W.H., 2019a, Map data from landslides triggered by Hurricane María in four study areas of Puerto Rico: U.S. Geological Survey data release. https://doi.org/10.5066/P9OW4SLX

Bessette-Kirton E.K., Cerovski-Darriau C., Schulz W.H., Coe J.A., Kean J.W., Godt J.W., Thomas M.A., Hughes K.S., 2019b, Landslides triggered by Hurricane María: assessment of an extreme event in Puerto Rico. GSA Today 29:4–10.

Brien, D.L., Reid, M.E., Cronkite-Ratcliff, C., and Perkins, J.P., 2021, Portraying runout and inundation from hurricane-induced landslides in Puerto Rico: Geological Society of America Abstracts with Programs. Vol 53, No. 6, 2021 doi: 10.1130/abs/2021AM-368632.

Hughes K.S., Bayouth-García D., Martínez-Milian G.O., Schulz W.H., Baum R.L. (2019) Map of slope-failure locations in Puerto Rico after Hurricane María: U.S. Geological Survey Data Release. https://doi. org/10.5066/P9BVMD74. Accessed 12 September 2019

Ho, J.-Y.; Lee, K.T.; Chang, T.-C.; Wang, Z.-Y.; and Liao, Y.-H., 2012, Influences of spatial distribution of soil thickness on shallow landslide prediction: Engineering Geology, Vol. 124, pp. 38–46.

Jolly W.T., Lidiak E.G., Dickin A.P., Wu Tsai-Way, 1998, Geochemical diversity of Mesozoic island arc tectonic blocks in eastern Puerto Rico. In: Likiak E.G., Larue D.K.(eds) Tectonics and geochemistry of the Northeastern Caribbean: Geological Society of America Special Paper vol. 322. p 67–98. https://doi.org/10.1130/0-8137-2322-1.67

Pelletier, J.D., and Rasmussen, C., 2009, Geomorphically based predictive mapping of soil thickness in upland watersheds: Water Resources Research, Vol. 45, W09417.

Tello, M., 2020, Optimization of landslide susceptibility modeling: a Puerto Rico case study: Master of Science Thesis, Colorado School of Mines, Golden, https://hdl.handle.net/11124/174137 (accessed July 2, 2021).

U.S. Geological Survey, 2018, USGS NED Original Product Resolution PR Puerto Rico 2015: http://nationalmap.gov/elevation.html.